



## Molecular Crystals and Liquid Crystals

Publication details, including instructions for authors and subscription information:

<http://www.tandfonline.com/loi/gmcl20>

### Characterization of Blue Sensitive Holographic Polymer Dispersed Liquid Crystal for Microholographic Data Storage

L. Criante<sup>a</sup>, F. Vita<sup>a</sup>, R. Castagna<sup>a</sup>, D. E. Lucchetta<sup>a</sup> & F. Simoni<sup>a</sup>

<sup>a</sup> Dipartimento di Fisica e Ingegneria dei Materiali e del Territorio and CNISM, Università Politecnica delle Marche, Ancona, Italy

Version of record first published: 22 Sep 2010

To cite this article: L. Criante, F. Vita, R. Castagna, D. E. Lucchetta & F. Simoni (2007): Characterization of Blue Sensitive Holographic Polymer Dispersed Liquid Crystal for Microholographic Data Storage, *Molecular Crystals and Liquid Crystals*, 465:1, 203-215

To link to this article: <http://dx.doi.org/10.1080/15421400701205941>

PLEASE SCROLL DOWN FOR ARTICLE

Full terms and conditions of use: <http://www.tandfonline.com/page/terms-and-conditions>

This article may be used for research, teaching, and private study purposes. Any substantial or systematic reproduction, redistribution, reselling, loan, sub-licensing, systematic supply, or distribution in any form to anyone is expressly forbidden.

The publisher does not give any warranty express or implied or make any representation that the contents will be complete or accurate or up to date. The accuracy of any instructions, formulae, and drug doses should be independently verified with primary sources. The publisher shall not be liable for any loss, actions, claims, proceedings, demand, or costs or damages whatsoever or howsoever caused arising directly or indirectly in connection with or arising out of the use of this material.

## Characterization of Blue Sensitive Holographic Polymer Dispersed Liquid Crystal for Microholographic Data Storage

**L. Criante**

**F. Vita**

**R. Castagna**

**D. E. Lucchetta**

**F. Simoni**

Dipartimento di Fisica e Ingegneria dei Materiali e del Territorio  
and CNISM, Università Politecnica delle Marche, Ancona, Italy

*We present the results of an extended investigation performed on holographic reflection gratings recorded in blue sensitive polymer dispersed liquid crystals in view of a possible application in optical data-storage. The analysis has been performed by means of real-time spectroscopy during the polymerization process. The analysis of transmission spectra during the recording process showed a fast photopolymerization, resulting in the rapid formation of a reflection peak. Gratings characterized by high spatial frequency ( $>7000$  lines/mm), high diffraction efficiency (up to 50%) and large refractive index modulation ( $\Delta n \sim 0.008$ ) have been obtained. Unfortunately, the monomer conversion into a polymer network is generally characterized by a strong packing, with a consequent reduction in volume (polymerization shrinkage). This phenomenon induces a significant blue-shift of the reflected wavelength. With the aim of better understanding and possibly reducing the shrinkage, a new high-sensitive experimental technique has been developed to measure shrinkage effects in multi-component polymeric mixtures.*

**Keywords:** optical storage; photopolymerization; shrinkage

This work has been supported by EU in the frame of STRP project **MICROHOLAS**. Address correspondence to L. Criante, Dipartimento di Fisica e Ingegneria dei Materiali e del Territorio and CNISM, Università Politecnica delle Marche and INFN-CNR, via Breccie Bianche, 60131 Ancona Italy. E-mail: l.criante@univpm.it

## 1. INTRODUCTION

An attractive feature of holographic optics is the possibility of achieving high-density optical storage by writing digital information in the form of micro-holograms recorded in the volume of a suitable photosensitive substrate. This approach can considerably improve the volume capacity, storage density, response time and lifetime of the next generation optical data-storage systems. To a great extent their performance is determined by the characteristics of the used materials. For this reason this has resulted in tremendous efforts in development of suitable photosensitive materials, ranging from inorganic crystals, like doped  $\text{LiNbO}_3$ ,  $\text{LiTaO}_3$ ,  $\text{KnbO}_3$ ,  $\text{Sn}_2\text{P}_2\text{S}_6$  and  $\text{Bi}_2\text{TeO}_5$ , to different types of photopolymers and composite materials.

To fulfill the requirements of a system for high-density data-storage, a high-sensitive material with good resolution and response time is desired. Recently many experiments have been focused on polymeric materials because of their high photosensitivity, achievable resolution, good signal-to-noise ratio, and easy processability.

In this framework, European Union funded the Microholas project [1], with the purpose of developing a new class of CD-like optical memories. In particular, the project aims at a huge increase of the disk capacity, by recording periodic nanostructures in the disk volume (Holographic DVD), rather than “digging pits” on the disk surface as in conventional CDs/DVDs. The main advantage of this approach is that it takes bit-oriented storage to the third dimension: using highly focused beams, it is possible to record multiple tracks at different depth in the disk volume. In addition, writing with a blue laser and by superimposing many holograms in the same spatial position (wavelength multiplexing) the disk capacity can in principle increase up to the threshold of TeraByte. Wavelength multiplexing allows a linear increase of the data density and also of the write/read rate with the number of wavelength used.

Holographic polymer dispersed liquid crystals (H-PDLCs) are a class of composite photosensitive materials widely investigated for the realization of nano-structured electro-optical devices (electrically driven switchable gratings [2]) recorded through conventional holographic techniques [3]. In these systems, a spatially modulated light distribution, obtained by the interference of two laser beams, initiates a non-uniform polymerization in a photosensitive pre-polymer/liquid crystal mixture. On the other hand, this spatially anisotropic polymerization induces a counter-diffusion process of the mixture components and their consequent phase-separation: while the monomers diffuse to the bright regions, the liquid crystal is forced to the dark regions by

the growing polymer network. The final structure consists in a periodic arrangement of alternating polymer-rich and liquid crystal-rich planes, characterized by a different refractive index [4]. It acts as a volume phase grating, whose pitch can be selected by using different recording angles and writing wavelengths.

In this article we report the realization of high resolution H-PDLC reflection gratings with blue laser light and their characterization for microholographic data storage. In order to verify how the grating macroscopic behavior is connected to the properties of microholograms used in bit-oriented data-storage systems, a real-time analysis of transmission spectra have been performed during the recording process. Since the kinetics of the photopolymerization process is very fast, the observed rapid formation of the reflection peak makes us trusting in obtaining a writing speed sufficiently high for the desired application. In addition, the measurement of other important optical parameters, like diffraction efficiency, losses, sensitivity, refractive index modulation, wavelength selectivity, let us to verify the actual possibility to use H-PDLC as photosensitive materials for holographic data storage. Finally, an extend investigation of the shrinkage occurring during photopolymerization has been performed.

## 2. EXPERIMENTAL PART

H-PDLC gratings were realized by curing a homogenous mixture of dipentaerythritol hydroxy penta-acrylate (DPHPA) monomer and BL038 liquid crystal (LC). The mixture was sensitized to blue light by adding a solution of Genocure CQ (by Rahn) and N-phenyl glycine (NPG) dissolved in a monofunctional, low viscosity monomer (1-vinyl-2-pyrrolidone, NVP). The mass ratio of monomer, LC and photoinitiator solution is 65:25:10.

The experimental setup used for writing holographic reflection gratings is sketched in Figure 1. It basically consists of an Ar-ion laser ( $\lambda = 457.9$  nm), whose beam passes through a beam expander and a spatial filter (S.F.) and is then split into two equal amplitude branches by a non-polarizing beam-splitter. The two generated beams are reflected by the mirrors M1 and impinge on the sample from the two opposite sides (nearly counter-propagating condition), at an incidence angle chosen to avoid the overlap in the transmission spectra of the laser scattered light with the Bragg reflection peak.

The mirrors M1 are mounted on motorized rotational stages to select the incidence angle, and consequently the spatial frequency of the recorded grating, with high accuracy and repeatability. The sample is held in vertical position (perpendicular to plane of incidence) by using

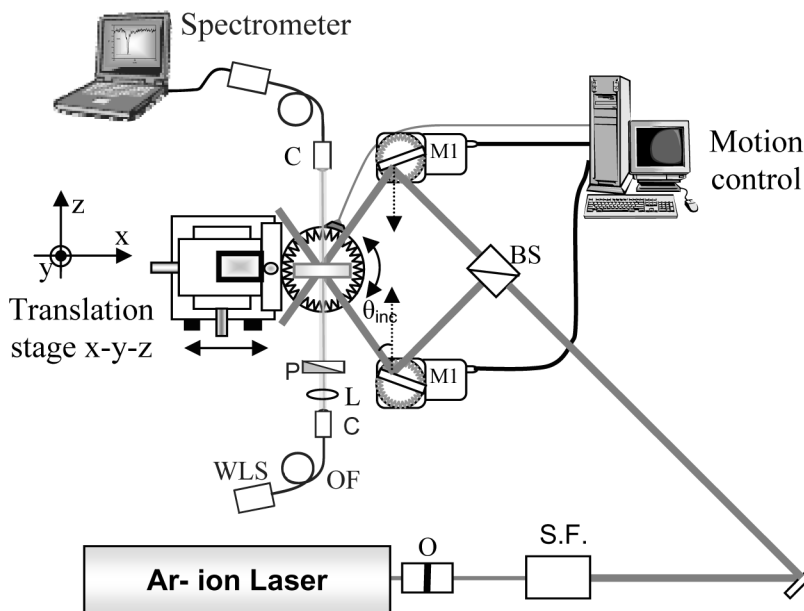


**FIGURE 1** Optical set-up for holographic recording: O shutter; SF spatial filter; M mirror; M1 motorized mirrors; BS beam splitter; WLS white light source; OF fiber optic; C collimator; L lens; P polarizer.

a tilting platform assembled on a motorized goniometer. Since our mixture used is not sensitive to red light, a He-Ne laser ( $\lambda = 632.8 \text{ nm}$ , not shown in Figure 1) is used for the accurate alignment of the sample.

For gratings studied in this work, the intensity of each writing laser beam was approximately  $I = 80 \text{ mW/cm}^2$ ; the incidence angle was fixed at  $\theta_{inc} = 14 \text{ deg}$ , in order to obtain a grating pitch as small as  $\Lambda_{th} \sim 0.150 \mu\text{m}$ .

While the polymerization is proceeding, the grating formation is monitored in real-time by measuring the sample transmittance: in fact, the appearance of a notch in the transmission spectrum is the clear signature of the growth of the grating. The measurement is performed by illuminating the grating with unpolarized broadband radiation ( $\lambda = 350 \div 1000 \text{ nm}$ ), emitted by an incoherent white light source (WLS) and carried by an optical fiber. The white beam impinges on the sample at normal incidence, and is then directed, by a second optical fiber, to a high resolution spectrometer (res.  $< 0.4 \text{ nm}$ ). The white beam spot size on the sample is about one third of the recording beam

diameter, which is 8 mm. The transmission spectra are digitally recorded and displayed on line by the computer, with a time resolution of 0.4 s. The same apparatus is also used after recording, to monitor the grating stability.

### 3. CHARACTERISTICS OF REFLECTION GRATINGS

At the end of the curing process a periodic structure made of alternating polymer-rich and liquid crystal-rich layers is obtained. Due to the mismatch of refractive index, this periodic arrangement acts as an efficient holographic mirror, whose reflectivity and angular selectivity depend on several experimental factors (i.e., refractive index modulation, optical losses, grating pitch and thickness).

The formation of the reflection peak and its wavelength shift are presented in Figure 2 at different times. The continuous curve, acquired after an exposure of  $t = 0.8$  s, shows the very first Bragg notch to appear after the shutter is opened. It corresponds to an initial low efficiency gratings, which rapidly grows in the following seconds. Finally, after an irradiation of  $t = 4.0$  s, the reflection notch reaches its maximum depth (dotted curve) and the exposure can be stopped.

This is clearly shown in Figure 3, where the grating diffraction efficiency  $\eta$  (the notch depth) and transparency (the transmittance of

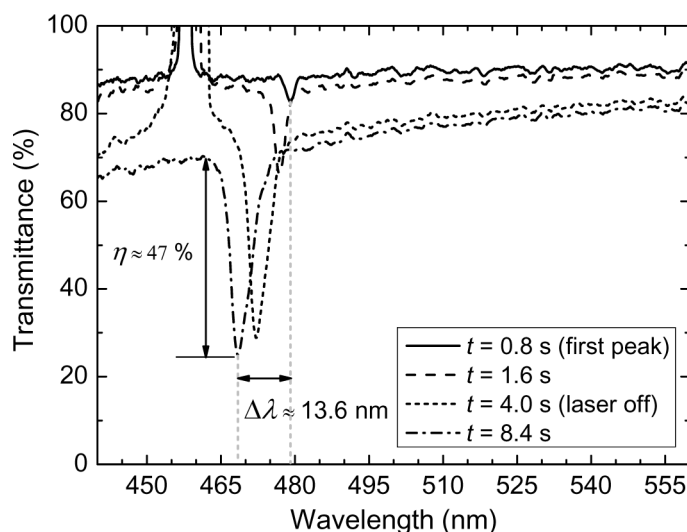


**FIGURE 2** Time evolution of the transmission spectra during the grating recording.

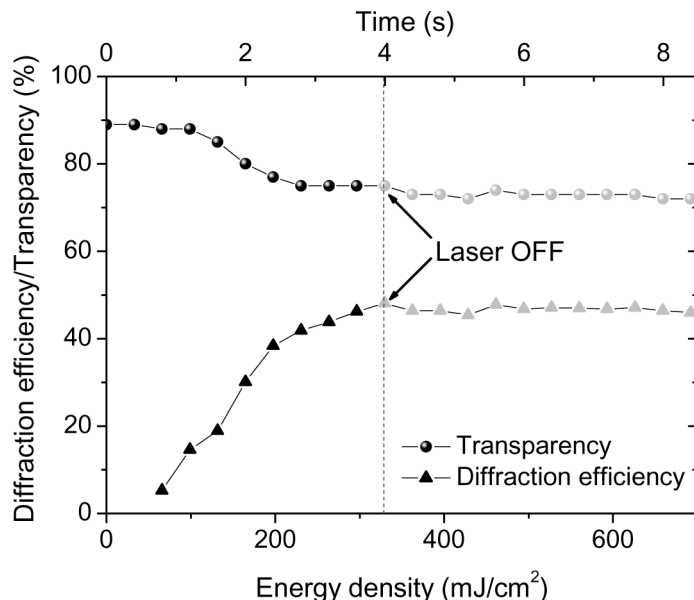


**FIGURE 3** Diffraction efficiency (triangles) and sample transparency (full spheres) as a function of writing energy density and time. Clearly, the energy scale is not relevant after the laser is switched off.

the spectrum baseline) are plotted as a function of the writing energy density. The formation dynamics appears characterized by an induction energy density ( $\sim 66 \text{ mJ/cm}^2$ ), necessary to trigger the polymerization; for further exposure, diffraction efficiency grows and stabilizes at a value of 47%, corresponding to an energy density of  $\sim 300 \text{ mJ/cm}^2$ . An opposite behavior is shown by the grating transparency: initially, the mixture is very transparent and the sample losses are almost totally caused by reflections at the glass surfaces; subsequently, when diffraction efficiency has reached  $\sim 20\%$ , transparency decreases to the final value of  $\sim 75\%$  (which still includes  $6\div 7\%$  glasses losses). This behavior is characteristic of H-PDLCs and is connected to the nucleation and growth of nematic LC droplets, large enough to produce a noticeable scattering. Transparency is a critical parameter for data storage application, and overall losses (absorption and scattering) should not exceed the limit value of  $20\div 25\%$ . In our materials this value can be controlled by carefully choosing the initial concentration of photoinitiators and liquid crystal in the photosensitive syrup.



It must be underlined that the goal of a system for optical data storage is to distinguish between the presence (bit 1) and the absence (bit 0) of a micrograting with a bit error rate (BER)  $< 10^{-4} \div 10^{-5}$ . Actually, it means that one needs not to write microgratings with a 50% efficiency: what is important is reaching a decision threshold that allows to correctly detect the recorded digital data. As a matter of fact,  $\eta = 0.1\%$  is a very large value for reflection microgratings. In order to characterize data-storage materials independently on the experimental conditions, which can vary with the testing apparatus, a new parameter, the sensitivity  $S$ , is commonly introduced. For reflection holograms it is defined as:

$$S = \frac{\sqrt{\eta}}{I t d} \text{ [cm/J]}, \quad (1)$$

where  $\eta$  is the diffraction efficiency,  $I$  the recording light intensity,  $t$  the exposure time and  $d$  the sample thickness. It is widely recognized as the most important parameter describing the performance of holographic materials. In our case, the kinetics of  $S$  during the recording process is represented in Figure 4. The obtained values almost reaches  $10^3$  cm/J, indicating that H-PDLCs are well suitable for holographic data storage applications.

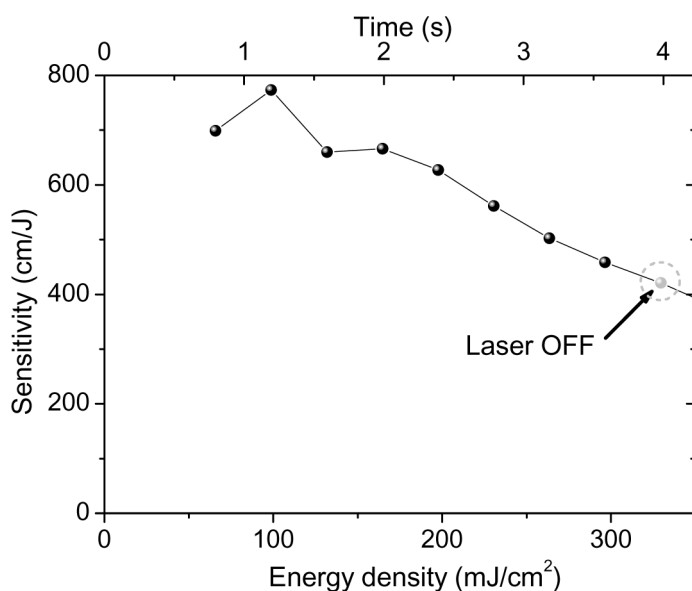


**FIGURE 4** Sensitivity of the mixture during the recording process.

The main advantage of holographic data storage is the possibility of increasing the disk capacity by superimposing different gratings, each one reflecting a slightly different wavelength. Consequently, the higher is the wavelength selectivity, defined as the full width at half maximum (FWHM) of the reflection peak, the more are the gratings that can be used for wavelength multiplexing. Figure 5 shows the growth of FWHM with the curing energy density. This behavior is similar to that one observed for diffraction efficiency, in agreement with the theory, which predicts a rise of both  $\eta$  and FWHM when the refractive index modulation increases. The final value of 4.5 nm demonstrates the very good selectivity of our H-PDLCs.

Another important feature that is evident in Figure 2 is the shift of the reflection peak towards shorter wavelengths while the polymerization proceeds. The horizontal bi-arrow in the graph indicates the reflected wavelength displacement observed during the time evolution of the photopolymerization process. This effect is always encountered in reflection gratings recorded in photopolymers and it is connected to the monomer conversion into a polymer network. This process is accompanied by a reduction in volume, commonly known as polymerization shrinkage ( $S$ ).

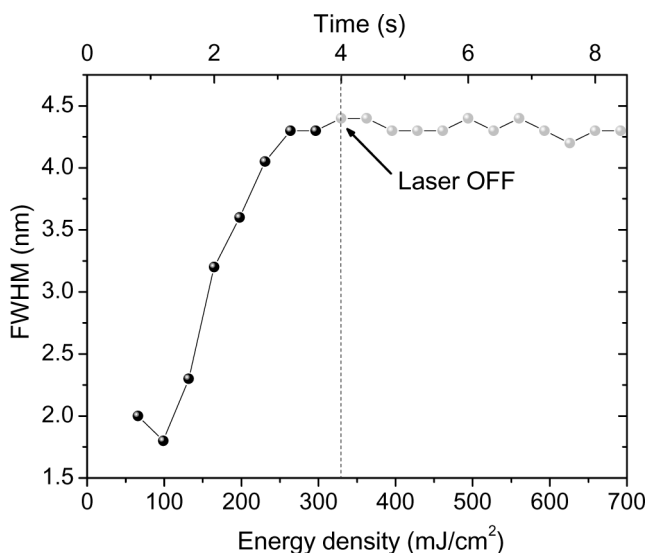


**FIGURE 5** Reflection peak Full Width at Half Maximum as function of writing energy density and time. As in Figure 3 the energy scale is not relevant after the laser is switched off.

In a reflection grating, the reflected wavelength  $\lambda_{Re}$  is determined, for normal incidence, by the well-known Bragg law

$$\lambda_{Re} = 2 n_{ave} \Lambda, \quad (2)$$

where  $n_{ave}$  is the grating average refractive index. Actually, polymerization shrinkage induces a change in both  $n_{ave}$  and  $\Lambda$ . Performing a finite element analysis, we can quantify the absolute wavelength displacement  $\Delta\lambda_{Re}$  of the experimental reflection wavelength  $\lambda_{Re-exp}$  with respect to theoretical reflection wavelength  $\lambda_{Re-th}$ , as defined by the geometrical writing conditions:

$$\Delta\lambda_{Re} = \lambda_{Re-th} - \lambda_{Re-exp} = 2(\Delta n_{ave} \cdot \Lambda + n_{ave} \cdot \Delta\Lambda). \quad (3)$$

Here  $\Delta n_{ave} = n_{ave-mix} - n_{ave-gr}$  is the difference between the average refractive index of the pre-polymer mixture and the average refractive index of the cured grating, while  $\Delta\Lambda = \Lambda_{th} - \Lambda_{exp}$  represents the difference between the theoretical pitch (defined by the recording geometry and measurable by observing the initial position of the notch, as soon as it is detected) and the effective notch recorded into the sample at the end of the photopolymerization process. In the following we define *optical shrinkage* the quantity  $S_{opt} = \Delta\lambda_{Re}/\lambda_{Re-th}$ , i.e., the relative change of the reflected wavelength, as measured by the spectrometer. From Eq. (3) it results

$$S_{opt} = \frac{\Delta\lambda}{\lambda_{Re-th}} = \frac{\Delta n_{ave}}{n_{ave-mix}} + \frac{\Delta\Lambda}{\Lambda_{th}}. \quad (4)$$

Here it is important to notice that the quantities  $\Delta n_{ave}$  and  $\Delta\Lambda$  have opposite signs: while  $\Delta\Lambda$  is positive (the grating mechanically shrinks),  $\Delta n_{ave}$  is negative, as the refractive index increases with the material density and is thus higher for polymer than for monomer. Then the two effects are in competition, the former inducing a blue-shift of the reflection notch, the latter inducing a red-shift. However the experimental evidence indicates they do not compensate each other, and a net blue-shift is typically observed. This means that the optical shrinkage is much more affected by the mechanical shrinkage  $S_{mech}$  (defined as  $\Delta\Lambda/\Lambda_{th}$ ) than by the relative change of the refractive index.

All this considered, the effective reflected wavelength can be calculated as a function of the writing wavelength  $\lambda_{write}$  and the external incidence angle of the recording beams  $\theta_{inc}$ , measured with respect to the normal of the grating:

$$\lambda_{Re-exp} = \frac{n_{ave-gr}}{n_{ave-mix}} \frac{(1 - S_{mech})\lambda_{write}}{\sqrt{(1 - [(\sin \theta_{inc})/n_{ave-mix}]^2)}}, \quad (5)$$

where the Snell's law has been used to link the external incidence angle with that one inside the sample. This expression can be conveniently used to predict the final notch position, once the properties of the material and the curing geometry is known. On the other hand, it can also be used to measure with high sensitivity the mechanical shrinkage of the polymer. This parameter, of great interest for many different applications, is typically measured with mechanical methods, inherently characterized by low precision and sensitivity. In contrast, our optical system can easily reach a nanometer sensitivity, provided the polymer under investigation is suitable for recording of a periodic structure.

The time evolution of the optical shrinkage is reported in Figure 6 as a function of energy density and time. During the curing process,  $S_{opt}$  increases almost linearly with the irradiation energy (or time), up to reaching the value of 1.5% at the end of the curing process (corresponding to a shift of about 10 nm). However, shrinkage continues, at a slower rate, even after the laser is switched off and the sample stored in darkness. It finally stops only after some days, when it reaches a steady value typically about 3%. This is probably connected

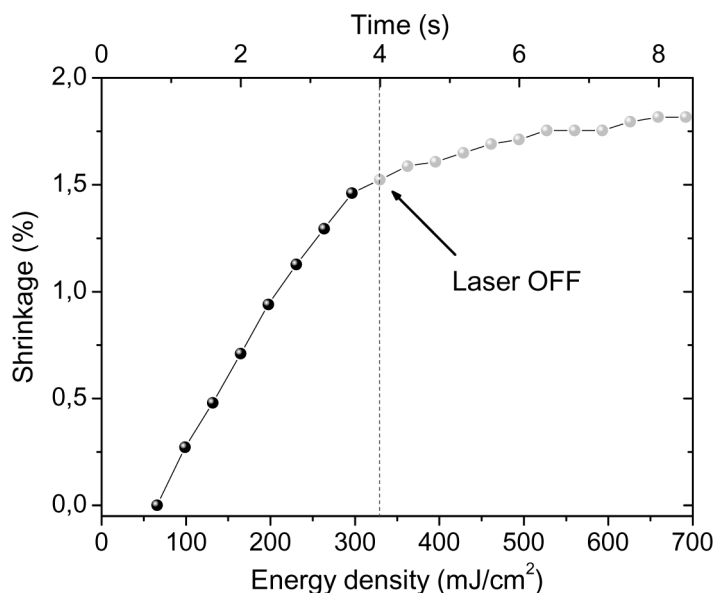


**FIGURE 6** Optical Shrinkage of the grating as function of energy density and time. As in Figure 3 the energy scale is not relevant after the laser is switched off.

to the presence of unreacted radicals which propagate the polymerization reaction even in absence of curing light.

In most practical circumstances shrinkage must be low, even if for microholography it is not so critical as for other applications. However, a way to control this undesired effect could be the addition of some radical scavenger into the mixture; our first experiments in this direction provided promising results reducing the long-term optical shrinkage of over 50%. Moreover, one must consider that the shrinkage is not only dependent on the degree of polymerization, but also on chemicals parameters like the monomer shape and the arrangement of the polymer chains.

When the stability conditions are fulfilled and the peak position is unchanged, the ability of the grating to select and reflect a narrow frequency band can be investigated. The value of the refractive index modulation (superimposed to  $n_{ave-gr}$ ) has been evaluated using the experimental technique described in ref [5]. The technique is based on the analysis of the displacement of the reflection notch, for the two standard polarizations ( $s$  and  $p$ ), due to small sample rotations. Each wavelength has its own Bragg angle and its corresponding value of diffraction efficiency. The minimum in each transmission spectrum gave us information on the Bragg-diffracted light. Changes in the amplitude and position of this peak were determined by the transmitted light and provided information about the diffraction efficiencies in reflection. By fitting this experimental data using the theory of Montemezzani *et al.* [6] we can determine the modulation value of the grating refractive index. As an example, the peak displacement for different incidence angles is reported in Figure 7 for  $p$  polarizations. The method, developed for H-PDLC samples showing small values of optical anisotropy [5], can be applied also in this case in order to evaluate the magnitude of the index modulation  $\Delta n$ . In our case we get  $\Delta n \sim 0.008$ .

In order to verify how the macroscopic behavior of gratings is connected to the properties of microholograms used in bit oriented data-storage system, the H-PDLC materials have also been tested in the microholographic setup, available at the Institute of Optics of the Technical University of Berlin (TUB). The work has been focused on the identification of the best exposure parameters (light intensity and exposure time) to obtain 3D microgratings with sufficiently high diffraction efficiency [7]. This analysis also allows the detection of the photosensitivity threshold of the material, i.e., the minimum amount of energy needed to write a readable hologram. By these experiments, it has been observed that the lower is the energy threshold, the smaller are the recorded microgratings. Therefore, a good

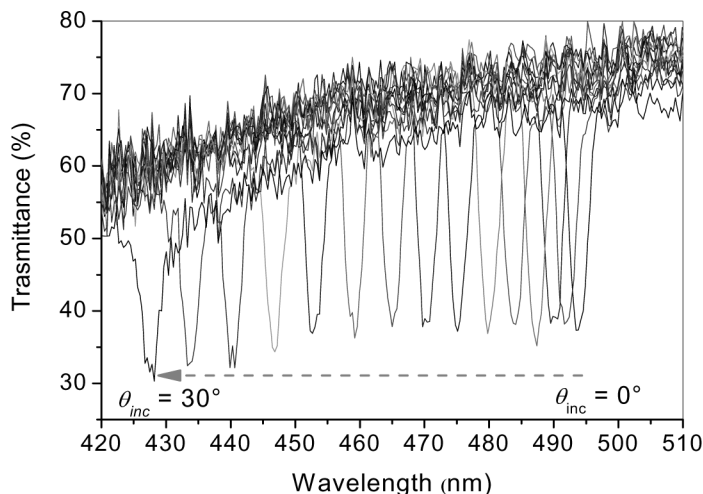


**FIGURE 7** Transmission spectra of the displacement of the reflection peak for different incidence angle for a p-polarized impinging light.

photosensitivity is fundamental to write closely packed holographic structures. In order to reach this important goal, it is therefore necessary to choose a writing energy density close to the material sensitivity threshold.

## CONCLUSIONS

Blue light sensitive H-PDLCs were investigated as suitable materials for holographic data storage applications, by means of real-time and post-curing spectroscopic analyses. Gratings characterized by a high spatial frequency ( $>7000$  lines/mm), a diffraction efficiency up to 50% and an index modulation  $\Delta n \sim 0.008$  have been obtained. The measured material sensitivity ( $S \sim 10^3$  cm/J) confirms the possibility of using these materials for high density optical storage applications, as also proved by measurements carried out with the micro-holographic setup. Finally, an accurate analysis of optical shrinkage pointed out the role of mechanical shrinkage compared to the change of refractive index induced by the grating formation.

## REFERENCES

- [1] European Project "Microholas," contract STRP n. 511437.
- [2] Sutherland, R. L., Tondiglia, V. P., Natarajan, L. V., Bunning, T. J., & Adams, W. W. (1994). *Appl. Phys. Lett.*, **64**, 1074.

- [3] Bunning, T., Natarajan, L. V., Tondiglia, V. P., & Sutherland, R. L. (2000). *Annu. Rev. Mater. Sci.*, 30, 83.
- [4] Sutherland, R. L., Natarajan, L. V., Tondiglia, V. P., & Bunning, T. J. (1993). *Chem. Mater.*, 5, 1533.
- [5] Lucchetta, D. E., Criante, L., & Simoni, F. (2003). *Optics Letters*, 28, 725.
- [6] Montemezzani, G. & Zgonik, M. (1997). *Phys. Rev. E*, 55, 1035.
- [7] Criante, L., Beev, K., Lucchetta, D. E., Simoni, F., Frohmann, S., & Orlic, S. (2005). *Proceedings of SPIE*, 5939, 61.